Collision-induced absorption by N2 near 2.16 μm: Calculations, model, and consequences for atmospheric remote sensing

J. -M. Hartmann, C. Boulet, G. C. Toon

RESEARCH ARTICLE

Key Points:
- Molecular dynamics simulations of the N_2-N_2 collision-induced absorption near 2.16 micrometers
- Semiempirical simple modeling of the N_2-air collision-induced absorption by N_2
- Successful comparisons with ground-based atmospheric transmission spectra

Collision-induced absorption by N_2 near 2.16 μm: Calculations, model, and consequences for atmospheric remote sensing

J.-M. Hartmann[1] (ID)**, C. Boulet**[2]**, and G. C. Toon**[3]

[1]Laboratoire de Météorologie Dynamique, CNRS/IPSL, Ecole polytechnique, Université Paris-Saclay, Palaiseau, France, [2]Institut des Sciences Moléculaires d'Orsay (ISMO), CNRS, Université Paris-Sud, Université Paris-Saclay, Orsay, France, [3]Jet Propulsion Laboratory, California Institute of Technology, Pasadena, California, USA

Abstract Classical molecular dynamics simulations (CMDS) are used for calculations of the collision-induced absorption (CIA) by pure N_2 in the (2.1–2.2 μm) region of the first overtone band. They lead to reasonable (±15%) agreement with the only two laboratory measurements available, at 97 K and room temperature. Based on these experiment/theory comparisons, empirical corrections are made to the CMDS-calculated CIA of pure N_2 in the 200–300 K temperature range. In addition, the contribution of N_2-O_2 collisions is, in the absence of any laboratory measurement, calculated and a simple semiempirical model (the first of its kind) is built in order to predict the CIA of N_2 under Earth atmosphere conditions. This is successfully validated by comparisons with ground-based atmospheric transmission spectra in the 2.1–2.2 μm region.

1. Introduction

It is now well known that collision-induced absorption (CIA) [*Frommhold*, 2006; *Hartmann et al.*, 2008] by nitrogen must be taken into account for the modeling of radiative processes and/or remote sensing studies in the atmospheres of the Earth and Titan, for instance. This has motivated many experimental and theoretical laboratory studies in the rototranslational and fundamental bands [e.g., *Bussery-Honvault and Hartmann*, 2014; *Karman et al.*, 2015; *Boissoles et al.*, 1994; *Menoux et al.*, 1993, and those cited therein] and has led to the inclusion of available data in the HITRAN database [*Richard et al.*, 2012]. In contrast, almost nothing has been done about the first overtone centered near 4630 cm^{-1} since only two very limited (pure N_2, 97 K, and room temperature) and old experimental studies are available [*Shapiro and Gush*, 1966; *McKellar*, 1989]. Furthermore, and to the best of our knowledge, no calculation has ever been made and atmospheric consequences have not been investigated so far. This situation and the fact that this band can be observed in our atmosphere (as shown in this paper) in a key region for the satellite remote sensing of CO_2 [*Crisp et al.*, 2004; *Boesch et al.*, 2011; *Hamazaki et al.*, 2005; *Buil et al.*, 2011] and for ground-based measurements of H_2O and N_2O [*Wunch et al.*, 2011] obviously justify the present study.

In this paper, the CIA in the 2-0 band region of N_2 around 2.16 μm is modeled using two approaches. In the first, classical molecular dynamics simulations (CMDS) are performed as done in [*Hartmann et al.*, 2011; *Bussery-Honvault and Hartmann*, 2014]. They lead to satisfactory agreement with the available laboratory measurements and enable the first quantitative analysis of the spectral contributions of "single" and "simultaneous" transitions in the considered band. However, since experiments are limited to two pure N_2 spectra recorded a long time ago [*Shapiro and Gush*, 1966; *McKellar*, 1989] and because the agreement between predictions and measurements is not sufficiently good for atmospheric applications, a semiempirical model is developed. For this, corrections of the CMDS-calculated N_2-N_2 CIA are made, based on experimental values, and the N_2-O_2 CIA is, in the absence of any measurement, calculated using CMDS. The resulting temperature-dependent CIA of N_2 in air is parameterized using a simple law suitable for easy calculations of atmospheric absorption. Based on this, comparisons are made with ground-based transmission spectra of the Earth atmosphere measured by the Jet Propulsion Laboratory (JPL) MkIV Fourier transform infrared (FTIR) spectrometer [*Toon*, 1991] from Esrange, Sweden. These show the importance of the absorption when large air masses are involved and demonstrate the quality of the proposed model.

The remainder of this paper is divided into five sections. In section 2, the CMDS approach is described together with the input data. Comparisons are made between its predictions and laboratory measured CIA spectra for pure N_2. In section 3, we generate data for calculations of the CIA in the 2-0 band region of N_2

in the Earth atmosphere. Comparisons between measured and calculated atmospheric spectra are presented and discussed in section 4 before the concluding remarks of section 5.

2. Calculations

The theoretical approaches available to calculate collision-induced absorption spectra can be divided into three groups [*Frommhold*, 2006; *Hartmann et al.*, 2008]. In the first one, based on the isotropic approximation, a rotational stick spectrum is calculated quantum mechanically and the (translational) broadening of each component is introduced using empirical line shape functions. A good example in the case of N_2 is given by *Boissoles et al.* [1994]. Alternatively, purely quantum calculations can also be performed, still within the isotropic approximation [*Borysow and Frommhold*, 1986] or, thanks to the increase of computer power, by taking into account the anisotropy of the intermolecular potential [*Karman et al.*, 2015]. Finally, classical molecular dynamics simulations (CMDS) can also be used, and they were successfully applied to the far infrared N_2 spectrum [*Bussery-Honvault and Hartmann*, 2014]. Note that, regardless of the model, no theoretical attempt to model the first overtone CIA band of N_2 has been made so far.

2.1. CMDS and Laboratory Data Used

The CMDS carried here are very similar to those used for calculations of the CO_2 [*Hartmann et al.*, 2011] and N_2 [*Bussery-Honvault and Hartmann*, 2014] far infrared CIA bands. Since details can be found in these references, only a brief summary is given below before describing the aspects specific to the present calculations. In the present CMDS, $\approx 10^6$ molecules have been considered, distributed in 48 cubic boxes treated in parallel with periodic boundary conditions [*Allen and Tildesley*, 1987]. The size of these boxes was determined from the retained density of 5 Am and the chosen temperature. The translational velocities and rotational angular momenta were initialized as randomly oriented vectors with modulus verifying the Maxwell-Boltzmann distributions. The orientations of the molecules axes were also randomly chosen in the planes perpendicular to their angular momenta. Finally, the positions of the centers of mass were random inside each box with the constraint that molecules should not be closer than 9 Å, in order to avoid unphysical situations with molecules too close to each other. Then, the translational and rotational dynamics of all molecules were treated classically, governed by an (input, see below) anisotropic intermolecular potential. This provides the positions and orientations of all molecules at all times. From these, the dipole induced in each molecule by its surrounding neighbors is calculated using (input) molecular properties (polarizabilities, electric multipoles, etc) [*Hartmann et al.*, 2011] or an ab initio-induced dipole surface [*Bussery-Honvault and Hartmann*, 2014]. The autocorrelation function (ACF) of the dipole is then straightforwardly obtained whose Fourier-Laplace transform yields the absorption spectrum. Note that the calculations were carried for a time interval of 28 ps with a step of a few femtoseconds but that time zero (for the calculation of the ACF $\left\langle \overrightarrow{\mu}(0).\overrightarrow{\mu}(t) \right\rangle$) was set at 25 ps. This delay is sufficiently large for the molecules to have "forgotten" the initially imposed (see above) distance of 9 Å. Indeed, checks show that the distributions of the rotational and translational energies are then extremely stable and in excellent agreement with the Maxwell-Boltzmann distribution (with associated temperatures varying by only 0.1 K from the input one). Finally, the 3 ps over which the ACF is computed is long enough for the latter to decrease to nearly zero and ensure no cutoff bias.

The N_2-N_2 intermolecular potential of *Bouanich* [1992], based on site-site Lennard-Jones interactions complemented by coulombic ones, has been used. Concerning the N_2-N_2 induced dipole, while some ab initio calculations of its surface have been made [*Lokshtanov et al.*, 2008; *Bussery-Honvault and Hartmann*, 2014; *Karman et al.*, 2015], no ready to use parametrization versus molecular coordinates exist for the 2-0 band. However, previous studies [*Bussery-Honvault and Hartmann*, 2014; *Boissoles et al.*, 1994] have shown that the most efficient induction mechanism is the quadrupolar one. Hence, the dipole moment has been limited here to its asymptotic long-range components due to the isotropic (α) and anisotropic (γ) polarizabilities of one molecule in the electric field caused by the quadrupolar (Θ) and hexadecapolar (Φ) moments of another one. Note that no empirical short-range component has been added and that, since all the needed molecular parameters are taken from independent sources (see below), the dipole moment used can be considered as the "best available long-range dipole moment." The associated radial components of its spherical expansion are given in *Hartmann et al.* [2011] and in section 4.7 of *Frommhold* [2006]. Then the components in the laboratory frame can be obtained from equations (1) and (2) of *Hartmann et al.* [2011].
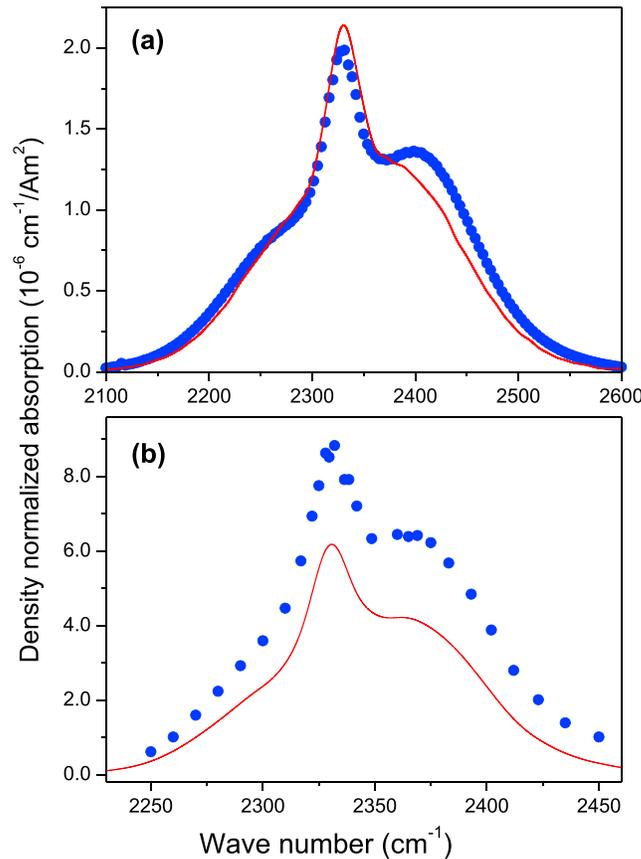
Table 1. Equilibrium Multipoles and Polarizabilities $P(0)$ of N_2, Their Derivatives $[d^kP/dx^k](0)$, and the Resulting Vibrational Transition Moments $\langle v|P(x)|v'\rangle$ (All in Atomic Units)[a]

	Quadrupole Θ	Hexadecapole Φ	Isotropic Polarizability α	Anisotropic Polarizability γ
$P(0)$	$-1.127(3)$	-6.8	11.85	4.6
$[dP/dx](0)$	$1.992(16)$	-5.56	12.81	14.58
$[d^2P/dx^2](0)$	0.92	24.44	7.91	16.64
$\langle 0|P(x)|0\rangle$	-1.133	-6.77	11.81	4.54
$\langle 0|P(x)|1\rangle$	5.83×10^{-2}	-0.158	0.375	0.428
$\langle 0|P(x)|2\rangle$	-2.68×10^{-3}	2.36×10^{-2}	-1.6×10^{-2}	-1.37×10^{-2}

[a]The numbers in parentheses are the uncertainties given in *Li and Le Roy* [2007]. The other parameters come from *Maroulis* [2003].

High level ab initio methods have been used to calculate the N_2 electric moments, polarizabilities, and their derivatives with respect to the bond length [*Lawson and Harrison*, 1997; *Maroulis*, 2003; *Li and Le Roy*, 2007]. Among the available data, we have principally retained those of *Maroulis* [2003] since this is the only work providing all the needed parameters computed in a self-consistent way. The quadrupole Θ and its first-order derivative were taken from a more recent calculation [*Li and Le Roy*, 2007]. The Taylor expansion of any molecular parameter $P(x)$ as function of the instantaneous reduced displacement from equilibrium, $x = (R - R_e)/R_e$, is written [*Maroulis*, 2003; *Li and Le Roy*, 2007] as follows:

$$P(x) = P(0) + \sum_{k=1,\infty} \frac{1}{k!}\frac{d^kP}{dx^k}(0) x^k. \qquad (1)$$

The equilibrium values $P(0)$ and their first-order and second-order derivatives are given in Table 1 together with the vibrational transition moments $\langle v|P(x)|v'\rangle$ needed for calculations in the 2-0 band region. To calculate the latter, the matrix elements of x^k given in *Tipping* [1973a, 1973b] were used, and the needed Dunham coefficients were taken in Table 1 of *Buldakov et al.* [2003].

2.2. Results for Pure N_2

For a preliminary test of our computations, we have simulated the CIA in the 1-0 band, which involves contributions of the $\langle 0|P(x)|0\rangle$ and $\langle 0|P(x)|1\rangle$ matrix elements of Table 1. As shown in Figure 1a, the comparisons between the resulting prediction and the room temperature measurements of *Lafferty et al.* [1996] and *Baranov et al.* [2005] lead to satisfactory agreement, with an overestimation of the peak absorption by about 10%. At low temperature, near 77 K, on the other hand, the CMDS underestimate the absorption by nearly 40%, as shown in Figure 1b (a similar result being obtained in the 0-0 band when compared with the measurements of *Wishnow et al.* [1996]).
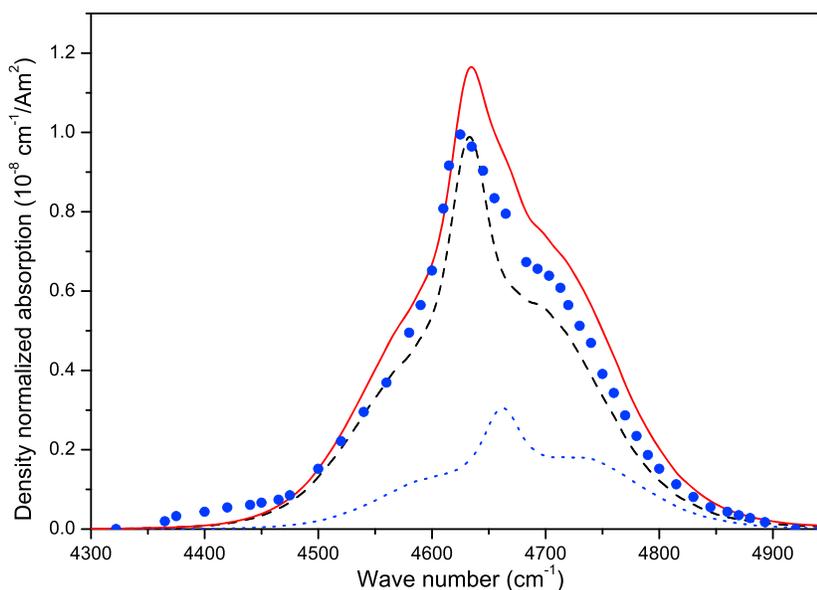

Figure 1. Measured (full blue circles) and calculated (lines) collision-induced absorptions in the fundamental band region of pure N_2 at the temperature of (a) 296 K with measured data from *Baranov et al.* [2005] and (b) 77 K with measured data from *McKellar* [1988].

Figure 2. Measured [*Shapiro and Gush*, 1966] (full blue circles) and calculated (lines) collision-induced absorptions in the first overtone band region of pure N_2 at room temperature. The blue dotted line and black dashed line are predictions for the double (twice 0-1) and single (0-2) collision-induced transitions, while the red line is the total obtained from their sum.

As shown below, the same behavior (overestimation at room T and too strong T dependence) is obtained for the 2-0 band.

As is well known, the absorption in the 2-0 band region of N_2 [*Shapiro and Gush*, 1966] (and more generally that in first overtone regions [*Hartmann et al.*, 2008]) results from two types of vibrational transitions: (1) Single transitions in which one N_2 molecule makes the $v = 0$ to $v = 2$ jump, while the other stays in the $v = 0$ level and only makes rotational transitions. The resulting spectrum, which peaks near $\sigma_{v=0 \rightarrow v=2} = 4631 \, \text{cm}^{-1}$, results from contributions of products $\langle 0|P(x)|2\rangle\langle 0|Q(x)|0\rangle$ where $P = \alpha$ or γ and $Q = \Theta$ or Φ or vice versa and (2) simultaneous or "double" transitions in which both molecules of a colliding pair simultaneously make a $v = 0$ to $v = 1$ jump. The resulting spectrum, which peaks near $2\sigma_{v=0 \rightarrow v=1} = 4660 \, \text{cm}^{-1}$ for pure N_2, results from contributions of products $\langle 0|P(x)|1\rangle\langle 0|Q(x)|1\rangle$ where $P = \alpha$ or γ and $Q = \Theta$ or Φ.

The single room temperature measured spectrum available in the 0-2 band region is reasonably well reproduced by the CMDS which, as in the 0-0 and 0-1 bands (see above), overestimate the peak absorption by about 10% (Figure 2). At this step, uncertainties on the intermolecular potential and/or the molecular parameters used may be invoked. Indeed, reducing all $\langle v|P(x)|v'\rangle$ values in Table 1 by 2.5% "mechanically" reduces the CIA spectrum by 10%. However, this explanation is insufficient in view of the low temperature results in Figure 3, which show, similarly to those obtained for the 0-0 and 1-0 bands, that the CMDS now underestimate the absorption (by about 15%). Our calculations thus overestimate the relative variations with temperature. Of course, part of that discrepancy may result from experimental sources, particularly for the first overtone since its absorption is very weak. From this point of view, new experiments in order to complete the only two ones available would be of considerable interest. The neglect of short-range-induced dipole components may be also invoked, and this should mostly [*Bussery-Honvault and Hartmann*, 2014; *Moreau et al.*, 2001] have effects at the higher temperature. Furthermore, a purely quantum calculation [e.g., *Karman et al.*, 2015] may be required since the classical description of the rotational dynamics, used here, may be quite approximate at (very) low temperature. In addition, the contributions of bound states, which have been identified in all N_2 CIA bands at low temperature [*McKellar*, 1988; *Wishnow et al.*, 1996; *McKellar*, 1989], may also be invoked. Indeed, shape resonances due to translational tunneling are completely absent from purely classical calculations as recalled in *Ivanov* [2004, 2016] for instance. On the opposite, such calculations intrinsically include "quasi-complexes" [*Ivanov*, 2016] which can lead to the formation of truly bound dimers if a third collision partner comes in with proper rotational and translational dynamics. At room
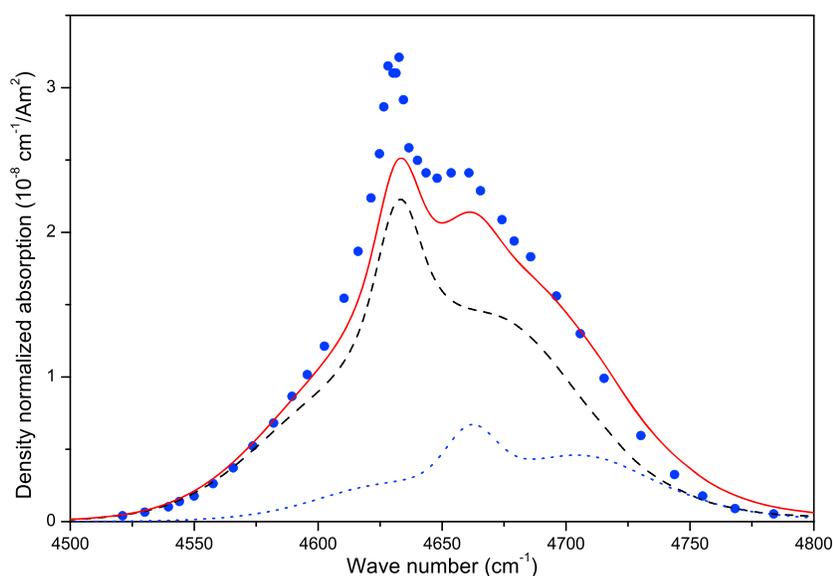
Figure 3. Same as Figure 2 but for the temperature of 97.5 K with measured absorptions from *McKellar* [1989].

temperature, the relative translational energy is significantly larger than the potential well depth, and the quantum effects missing in the CMDS likely make a small contribution to the spectra. On the opposite, they probably significantly participate to the absorption around 80 K, a possible explanation of the results in Figures 1a and 3. However, this is not a crucial issue for the present study for two reasons. The first is that empirical corrections are made to the CMDS-calculated results (see section 3). The second is that the application we make (section 4), which is the motivation of this work, is the simulation of N_2 absorption in the Earth atmosphere. Now the latter involves temperature above 200 K with main contributions to the absorption coming from layers warmer than 250 K, far away from the low values in Figures 1b and 3.

Finally, Figures 2 and 3 enable the first analysis of the respective spectral contributions of the single and double transitions, showing that the latter cannot be neglected. According to our calculations, it participates for about 25% to the overall spectrum area at room temperature and modifies the spectral shape due to its blue shift with respect to the single transition. Note that a relative contribution of 45% was estimated in *Shapiro and Gush* [1966] from an oversimplified analysis assuming a purely quadrupolar induction mechanism.

Finally, note that the sensitivity of CIA predictions to the intermolecular potential used is well known and that that used here for N_2-N_2 [*Bouanich*, 1992] may be oversimplified. It was however retained for two conjugated reasons after tests made using a more recent and accurate one [*Gomez et al.*, 2007]. The first is that the results obtained, although different (by typically 5–10%), still do not match the measurements and need empirical corrections. The second is that using this more refined potential leads to a very significant increase of the computational cost.

2.3. Predictions for N_2-O_2

Since we wish to model the absorption by N_2 in atmospheric air and that the latter contains oxygen, the CIA in the 2-0 band region of N_2 induced by collisions with O_2 must also be taken into account. In the absence (to our knowledge) of any measurement, CMDS were used to predict values at 200, 250, and 296 K. For the dynamics, the N_2-O_2 intermolecular potential was constructed from the N_2-N_2 and O_2-O_2 site-site Lennard-Jones interactions of *Bouanich* [1992] and complemented by coulombic ones. For the induced dipole, we used the values of $\langle 0|P(x)|2\rangle$ given in Table 1 for N_2 and, for O_2 [*Moreau et al.*, 2000]: $\langle 0|\Theta|0\rangle = -0.264$, $\langle 0|\Phi|0\rangle = 4.4$, $\langle 0|\alpha|0\rangle = 10.87$, and $\langle 0|\gamma|0\rangle = 7.3$, all in atomic units. Note that only the single transitions in which N_2 makes the $v=0$ to $v=2$ jump, while O_2 stays in the vibrational ground state is relevant. Indeed, double transitions in which both molecules makes a $v=0$ to $v=1$ jump would appear in a different spectral range, near $\sigma_{v=0\rightarrow v=1}^{N_2} + \sigma_{v=0\rightarrow v=1}^{O_2} = 3886\ cm^{-1}$. The resulting calculated N_2-O_2 CIA (not shown) looks very much
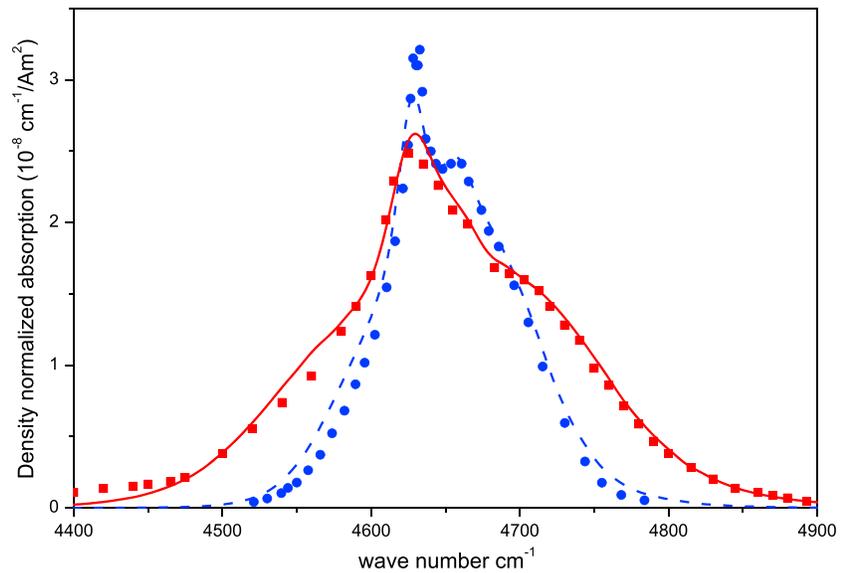
Figure 4. Comparison between the measured pure N_2 CIA at 97.5 K [*McKellar*, 1989] (blue circles) and room temperature [*Shapiro and Gush*, 1966] (values multiplied by 2.5, red squares) with the corresponding empirically corrected (see text) CMDS predictions (blue dashed line and red line, respectively).

alike the single transition spectrum of pure N_2 (e.g., Figure 2). It is only slightly less intense and narrower, results that can be explained by differences between the O_2 and N_2 molecular parameters.

3. Semiempirical Model for the 2-0 Band Region of N_2 in Air

For practical applications to radiative transfer and remote sensing in the Earth atmosphere, one needs a simple and accurate model of the CIA of N_2 in air (78%N_2 + 21%O_2) for temperatures between typically 200 and 300 K. We here explain how, based on both the CMDS predictions and available measurements, we have generated such a model and associated data.

We start from the results of Figures 2 and 3 and apply a purely empirical temperature-dependent multiplicative factor $f(T)$ to the CMDS predictions in order try to match the measured values. Assuming that $f(T)$ varies linearly with temperature, we obtain $f(T) = 0.9 + 0.00125(296 - T)$ from the results in Figures 2 and 3. The a priori choice of a linear function was made for two reasons. The first is that we have experiments at two temperatures only, imposing the use of a two-parameter empirical correction law. The second is that the temperatures of the atmospheric layers (those below typically 10 km, where the pressures P are the highest) which make the dominant contribution (through the P^2 dependence of the CIA) to the atmospheric absorption involve a relatively narrow range of temperature, typically between 250 and 300 K. Hence, the correction factors $f(T)$ involved take values close to $f(296 \text{ K}) = 0.9$ [e.g., $f(250 \text{ K}) = 0.95$ with the retained function] and are not too sensitive to the functional form of $f(T)$. In addition, a spectral shift of -5 cm^{-1} was applied to calculated values, corresponding to a compromise between the shifts between measured and calculated spectra at room temperature and 97.5 K. Applying these two corrections to CMDS predictions leads to a quite reasonable agreement with the available experiments for pure N_2, as shown by Figure 4. We then carried CMDS, still for pure N_2, at 200 K and 250 K and corrected them as explained above. This provides "good" values of the N_2-N_2 CIA in the 2-0 band region at 200, 250, and 296 K, including the contributions of single and double transitions.

The N_2-N_2 (CMDS + corrections) and N_2-O_2 (CMDS) results were then combined to yield CIA values for N_2 in air (78%N_2 + 21%O_2 + 1%Ar) through the following:

$$\text{CIA}^{N_2 \text{ in air}}(\sigma, T) = 0.78 f(T) \text{CIA}^{\text{CMDS } N_2-N_2}(\sigma, T) + 0.22 \text{CIA}^{\text{CMDS } N_2-O_2}(\sigma, T), \quad (2)$$

where σ is the wave number. Note that this assumes that the CMDS predictions for N_2-O_2 are close to the true values, a practically unavoidable choice in the absence of any measurements. Hence, although an interesting issue, estimating the accuracy of equation (2) is difficult, especially since the accuracy of the measurements is

not discussed in *Shapiro and Gush* [1966]. However, the results of section 4 indicate that 5% is a conservative estimate. Equation (2) also assumes that the N_2-Ar and N_2-O_2 CIA are identical, an approximation of small consequences considering the small relative amount of argon in atmospheric air. Finally, as done in [*Lafferty et al.*, 1996], the temperature dependence was parameterized using the simple law as follows:

$$CIA^{N_2 \text{ in air}}(\sigma, T) = B_0(\sigma)\exp[\beta(\sigma)[1/T_0 - 1/T]], \qquad (3)$$

with $T_0 = 296$ K. The two parameters $B_0(\sigma)$ and $\beta(\sigma)$ were deduced from a fit of the values obtained from equation (2) at 200, 250, and 296 K. These three temperatures cover the atmospheric range and are sufficient for the determination of the two parameters of equation (3). A posteriori checks show that equation (3) enables representation of the input CIA spectra within better than 5%. The values of $B_0(\sigma)$ and $\beta(\sigma)$, tabulated between 4300 and 5000 cm^{-1} with a 1 cm^{-1} step, and some Fortran routines for easy calculations of the CIA of N_2 in air are given as supporting information to this paper and/or available upon request to J.M.H.

4. Comparisons With Atmospheric Spectra

Figure 5 compares a ground-based atmospheric spectrum measured from Esrange, Sweden, on 22 January 2000, by the JPL MkIV Fourier Transform Spectrometer [*Toon*, 1991] with a calculation that included the N_2 CIA based on equation (3). The ground-based spectrum had first been ratioed against a MkIV balloon-borne solar spectrum measured in 2007 from 40 km altitude, in order to remove instrumental and solar features. This is important when fitting such a wide spectral interval; otherwise, unknown spectral variations in the solar or instrument response (e.g., due to detectors and filters) are difficult to distinguish from broad telluric absorptions. The HITRAN 2012 line list [*Rothman et al.*, 2013] was used throughout, except for the N_2 CIA, for which the above mentioned Fortran subroutines were used. Figure 5 (bottom) shows the spectral fit after scaling the vmr profiles of atmospheric N_2, CH_4, H_2O, CO_2, N_2O, and O_3, whose contributions to the total transmittance are color coded. Two scalars were also retrieved: the continuum level and the frequency shift. No higher-order continuum terms (tilt, curvature) were fitted nor any solar features since this spectrum had been ratioed. The next panel up zooms into the 80–100% transmittance range, showing the measured spectrum (black diamonds), the calculated total transmittance (black line), and the N_2 absorption alone (red). The discrete N_2 lines are quadrupole lines from HITRAN 2012 [*Rothman et al.*, 2013]. The broad continuum is from the N_2 CIA parameterization from this work. Figure 5 (second from top) shows the residuals (measured minus calculated) resulting from the fits with the N_2 CIA. The peak residuals are just over 2% and arise primarily from systematic errors in the assumed shape of the H_2O vmr profile. The noise level is about 0.3%, and the overall RMS residual is 0.46%. Figure 5 (top) shows the residuals resulting from a fit without the N_2 CIA (but still with the N_2 quadrupole lines). The residuals, which now have a 1.66% RMS and peaks exceeding 7%, reveal spectral signatures due to the improper fits of various gas absorptions. It is the case, for instance, near 4667 cm^{-1}, in the R branch of the O_3 band centered at 4655 cm^{-1}. This particular spectrum was chosen due to its high solar zenith angle (89.16°), low altitude (0.27 km), and low H_2O absorption (the spectrum was measured at −23°C and 43% relative humidity), maximizing the N_2 absorption contribution relative to that from other gases. Despite this, the N_2 CIA is only 11% deep and difficult to discern behind the much stronger absorptions of the other gases. The N_2O band centered at 4731 cm^{-1} (green) is one of the two used by the Total Carbon Column Observing Network (TCCON) network for ground-based measurements of column N_2O. Six of the TCCON H_2O windows, centered at 4565, 4572, 4577, 4611, 4622, and 4699 cm^{-1}, are located in the plotted window and will therefore be affected by the N_2 CIA parameterization. A full list of TCCON windows can be found at tccon-wiki.caltech.edu/index.php?title = Network_Policy/Data_Use_Policy/Data_Description_GGG2014&highlight = GGG2014.

We also fitted other MkIV atmospheric spectra, observed at slightly lower air masses (i.e., smaller solar zenith angles) and in other years than the one shown in Figure 5. From these fits we retrieved N_2 dry-air mole fractions. Figure 6 shows the retrieved N_2 mole fractions for 34 spectra measured on six different days in January of 2000, 2006, and 2007, plotted against their solar zenith angle (left) and air mass (right). The spectrum featured in Figure 5, representing 89.16° solar zenith angle or 25 air masses, is represented by the dark blue diamond point on the far right of Figure 6. The mean N_2 value for these 34 spectra was 0.783 ± 0.022. The closeness of this value to the truth (0.7809) and the lack of any significant air mass dependence imply that the
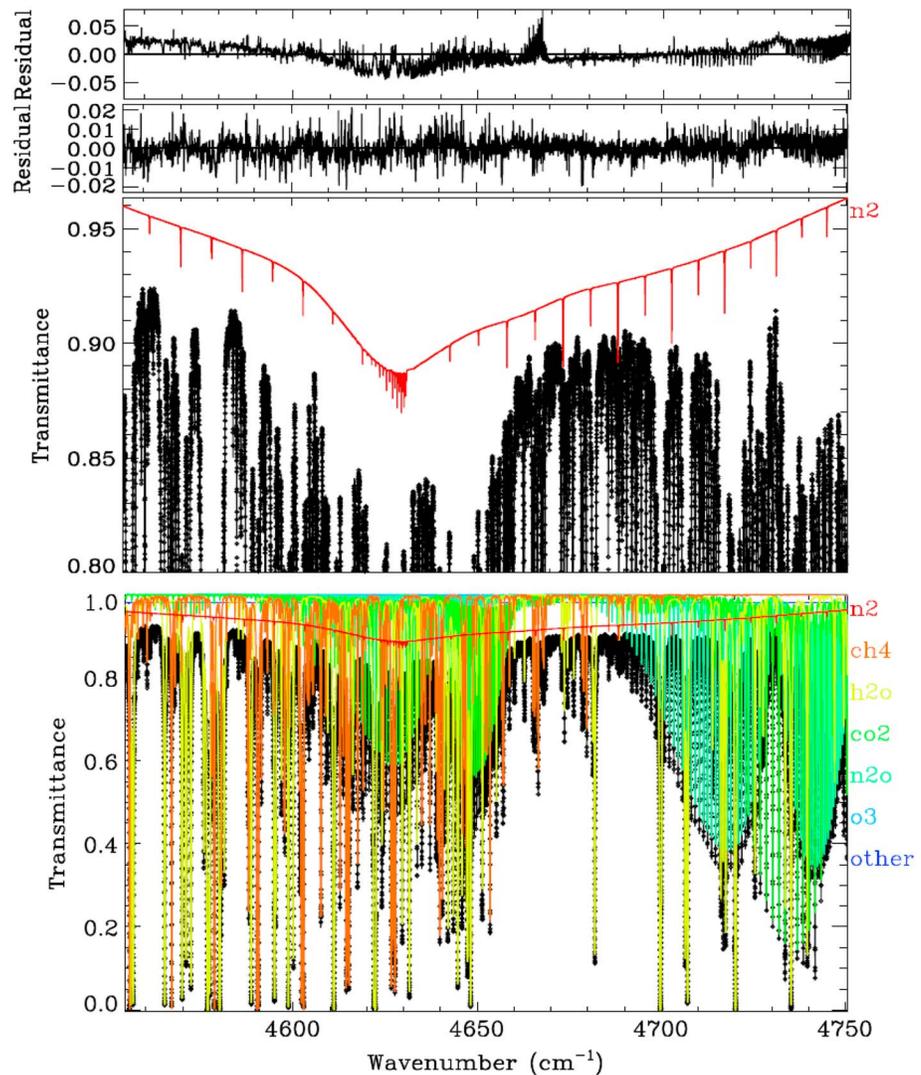
Figure 5. Comparison of a measured spectrum with a fitted calculation. Spectral fits to a ground-based atmospheric transmittance spectrum measured from Esrange, Sweden, on 22 January 2000 at a solar zenith angle of 89.16°. (bottom) The measured spectrum (black diamonds) and the absorption contributions of the various gases (colors). (middle, bottom) Zooming into the absorption contribution from N_2 alone (red). (middle, top) The residuals when the N_2 CIA is included from the calculation. (top) Residuals when N_2 CIA is excluded. Note the scale change between the top two panels.

proposed N_2 CIA spectroscopy is providing a very good representation of the N_2 absorption. For example, if the dip in the residuals in Figure 5 (top) from 4610 to 4640 cm^{-1} was partly due to an artifact in the spectral response of the MkIV instrument, then this would impart an air mass-dependent bias to the retrieved N_2 values.

The main importance of this work is not for better knowledge of the atmospheric N_2 amount but for more accurate retrievals of other gases that overlap the considered N_2 CIA band. For example, N_2O is retrieved by TCCON from two bands including the one centered at 4731 cm^{-1}. H_2O is retrieved from windows at 4565, 4570, 4572, 4577, 4599, 4611, 4622, and 4699 cm^{-1}. CO_2 is retrieved from a window centered at 4850 cm^{-1}, which is also used for the remote sensing of carbon dioxide from space [*Crisp et al.*, 2004; *Hamazaki et al.*, 2005; *Buil et al.*, 2011; *Boesch et al.*, 2011].

In order to quantify the influence of the N_2 CIA band, N_2O retrievals were performed using the TCCON-defined window centered at 4719.5 cm^{-1}. The retrieved N_2O was found to change by ~2.0%, depending on whether
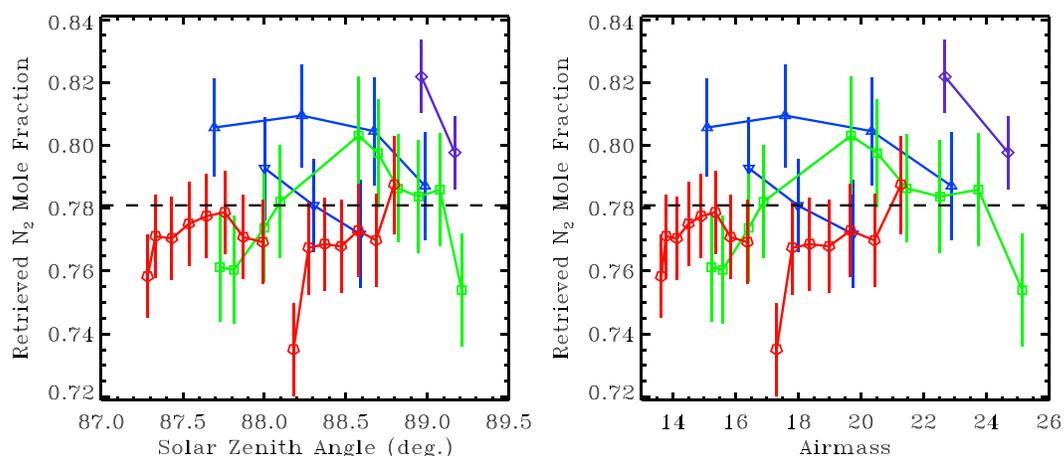
Figure 6. N_2 column-averaged dry-air mole fractions retrieved from 34 ground-based MkIV spectra measured on six different days in January 2000 (blue), 2006 (green), and 2007 (red) from Esrange, Sweden. The same N_2 retrievals are plotted in both panels, versus (left) solar zenith angle and versus (right) air mass. Most of the points fall within their error bars of the true N_2 mole fraction (0.7809), which is denoted by the black dashed line.

the N_2 CIA absorption was included in the forward model, for retrievals that fitted the continuum level, but not the tilt or curvature. As higher-order continuum contributions were included, then the N_2 CIA made less and less of an impact on the N_2O retrieval, because the continuum fit became able to mimic the shape of the N_2 CIA. But it is not a good retrieval strategy to mimic an air mass-dependent absorption feature with a set of parameters designed to represent the (air mass-independent) instrument response. CO_2 retrievals were performed using a $120\,cm^{-1}$ wide window centered at $4852\,cm^{-1}$. Using the N_2, CIA increased the retrieved CO_2 by 0.02% at 70° solar zenith angle (SZA), and by -0.04% at 89°, as compared with ignoring the N_2 CIA. These values are much smaller than for the $4719\,cm^{-1}$ N_2O window due to the small amount of overlap between the considered CO_2 band and the N_2 CIA absorption. Finally, like for N_2O, the effect of ignoring the N_2 CIA on the CO_2 retrieval decreases as more continuum parameters are fitted.

5. Conclusion

The N_2 CIA absorption centered around $4640\,cm^{-1}$ has been parameterized for the first time, based on classical molecular dynamics simulations (CMDS) and available measurements. The resulting FORTRAN subroutines were then used in performing spectral fits to high air mass, ground-based, solar absorption spectra measured by the JPL MkIV FTIR spectrometer from Esrange, Sweden. These spectra were chosen because of their high air mass, high atmospheric pressure, and dryness, which help emphasize the CIA absorption feature, in comparison with other absorptions. The spectral fits performed with the N_2 CIA contribution showed a large improvement in the fitting residuals, as compared with ignoring the N_2 CIA. The atmospheric N_2 mole fractions retrieved from spectra measured at SZA $> 87°$ were 0.783 ± 0.022, which is consistent with the known value of 0.7809. In addition, we have shown that the quality of the description of N_2 absorption can significantly impact the amounts of other molecules retrieved from atmospheric spectra around 2.16 μm.

References

Allen, M. P., and D. J. Tildesley (1987), *Computer Simulation of Liquids*, pp. 71–108, Clarendon Press, Oxford.
Baranov, Y. J., W. J. Lafferty, and G. T. Fraser (2005), Investigation of collision-induced absorption in the vibrational fundamental bands of O_2 and N_2 at elevated temperatures, *J. Mol. Spectrosc.*, *233*, 160–163.
Boesch, H., D. Baker, B. Connor, D. Crisp, and C. Miller (2011), Global characterization of CO_2 column retrievals from shortwave-infrared satellite observations of the Orbiting Carbon Observatory-2 mission, *Remote Sens.*, *3*, 270–304.
Boissoles, J., R. H. Tipping, and C. Boulet (1994), Theoretical study of the collision-induced fundamental absorption spectra of N_2-N_2 pairs for temperatures between 77 and 297 K, *J. Quant. Spectrosc. Radiat. Transfer*, *51*, 615–627.
Borysow, A., and L. Frommhold (1986), Collision induced rototranslational absorption spectra of N_2-N_2 pairs for temperatures from 50 to 300 K, *Astrophys. J.*, *311*, 1043–1057.
Bouanich, J. P. (1992), Site-site Lennard-Jones potential parameters for N_2, O_2, H_2, CO and CO_2, *J. Quant. Spectrosc. Radiat. Transfer*, *47*, 243–250.

Buil, C., V. Pascal, J. Loesel, C. Pierangelo, L. Roucayrol, and L. Tauziede (2011), A new space instrumental concept for the measurement of CO_2 concentration in the atmosphere, *Proc. SPIE*, *8176*, 817,621.

Buldakov, M. A., V. N. Cherepanov, B. V. Korolev, and I. I. Matrosov (2003), Role of intramolecular interactions in Raman spectra of N_2 and O_2 molecules, *J. Mol. Spectrosc.*, *217*, 1–8.

Bussery-Honvault, B., and J.-M. Hartmann (2014), Ab initio calculations for the far infrared collision induced absorption by N_2 gas, *J. Chem. Phys.*, *140*, 054,309.

Crisp, D., R. M. Atlas, F.-M. Breon, L. R. Brown, J. P. Burrows, P. Ciais, B. J. Connor, S. C. Doney, I. Y. Fung, and D. J. Jacob (2004), The Orbiting Carbon Observatory (OCO) mission, *Adv. Space Res.*, *34*, 700–709.

Frommhold, L. (2006), *Collision Induced Absorption in Gases*, Cambridge Monographs on Atomic, Molecular, and Chemical Physics, pp. 279–364, Cambridge Univ. Press, Cambridge.

Gomez, L., B. Bussery-Honvault, T. Cauchy, M. Bartolomei, D. Cappelletti, and F. Pirani (2007), Global fits of new intermolecular ground state potential energy surfaces for N_2-H_2 and N_2-N_2 van der Waals dimers, *Chem. Phys. Lett.*, *445*, 99–107.

Hamazaki, T., Y. Kaneko, A. Kuze, and K. Kondo (2005), Fourier transform spectrometer for Greenhouse Gases Observing Satellite (GOSAT), *Proc. SPIE*, *5659*, 73–80.

Hartmann, J.-M., C. Boulet, and D. Robert (2008), *Collisional Effects on Molecular Spectra. Laboratory Experiments and Model, Consequences for Applications*, pp. 275–301, Elsevier, Amsterdam.

Hartmann, J.-M., C. Boulet, and D. Jacquemart (2011), Molecular dynamics simulations for CO_2 absorption spectra. II. The far infrared collision-induced absorption band, *J. Chem. Phys.*, *134*, 094316.

Ivanov, S. V. (2004), Peculiarities of atom–quasidiatom collision complex formation: Classical trajectory study, *Mol. Phys.*, *102*, 1871–1880.

Ivanov, S. V. (2016), Quasi-bound complexes in collisions of different linear molecules: Classical trajectory study of their manifestations in rotational relaxation and spectral line broadening, *J. Quant. Spectrosc. Radiat. Transfer*, *177*, 269–282.

Karman, T., E. Miliordos, K. L. C. Hunt, G. C. Groenenboom, and A. Van der Avoird (2015), Quantum mechanical calculation of the collision-induced absorption spectra of N_2-N_2 with anisotropic interactions, *J. Chem. Phys.*, *142*, 084,306.

Lafferty, W. J., A. M. Solodoc, A. Weber, W. B. Olson, and J.-M. Hartmann (1996), Infrared collision-induced absorption by N_2 near 4.3 μm for atmospheric applications: Measurements and empirical modeling, *Appl. Opt.*, *35*, 5911–5917.

Lawson, D. B., and J. F. Harrison (1997), Distance dependence and spatial distribution of the molecular quadrupole moments of H_2, N_2, O_2, and F_2, *J. Phys. Chem. A*, *101*, 4781–4792.

Li, H., and R. J. Le Roy (2007), Quadrupole moment function and absolute infrared quadrupolar intensities for N_2, *J. Chem. Phys.*, *126*, 224,301.

Lokshtanov, S. E., B. Bussery-Honvault, and A. A. Vigasin (2008), Extensive ab initio study of the integrated IR intensity in the N_2 fundamental collision-induced band, *Mol. Phys.*, *106*, 1227–1231.

Maroulis, G. (2003), Accurate electric multipole moment, static polarizability and hyperpolarizability derivatives for N_2, *J. Chem. Phys.*, *118*, 2673–2687.

McKellar, A. R. W. (1988), Infrared spectra of the $(N_2)_2$ and N_2-Ar van der Waals molecules, *J. Chem. Phys.*, *88*, 4190–4196.

McKellar, A. R. W. (1989), Low-temperature infrared absorption of gaseous N_2 and N_2 + H_2 in the 2.0–2.5 μm region: Application to the atmospheres of Titan and Triton, *Icarus*, *80*, 361–369.

Menoux, V., R. Le Doucen, C. Boulet, A. Roblin, and A. M. Bouchardy (1993), Collision-induced absorption in the fundamental band of N_2: Temperature dependence of the absorption for N_2–N_2 and N_2–O_2 pairs, *Appl. Opt.*, *32*, 263–268.

Moreau, G., J. Boissoles, C. Boulet, R. H. Tipping, and Q. Ma (2000), Theoretical study of the collision-induced fundamental absorption spectra of O_2-O_2 pairs for temperatures between 193 and 273 K, *J. Quant. Spectrosc. Radiat. Transfer*, *64*, 87–107.

Moreau, G., J. Boissoles, R. LeDoucen, C. Boulet, R. H. Tipping, and Q. Ma (2001), Experimental and theoretical study of the collision-induced fundamental absorption spectra of N_2-O_2 and O_2-N_2 pairs, *J. Quant. Spectrosc. Radiat. Transfer*, *69*, 245–256.

Richard, C., et al. (2012), New section of the HITRAN database: Collision-Induced Absorption (CIA), *J. Quant. Spectrosc. Radiat. Transfer*, *113*, 1273–1285.

Rothman, L. S., et al. (2013), The HITRAN 2012 molecular spectroscopic database", *J. Quant. Spectrosc. Radiat. Transfer*, *130*, 4–50.

Shapiro, M. M., and H. P. Gush (1966), The collision-induced fundamental and first overtone bands of oxygen and nitrogen, *Can. J. Phys.*, *44*, 949–963.

Tipping, R. H. (1973a), Accurate analytic expectation values for an anharmonic oscillator using the hypervirial theorem, *J. Chem. Phys.*, *59*, 6433–6442.

Tipping, R. H. (1973b), Accurate analytic matrix elements for anharmonic oscillators using quantum mechanical commutator relations and sum rules, *J. Chem. Phys.*, *59*, 6443–6449.

Toon, G. C. (1991), The JPL MkIV interferometer, *Opt. Photonics News*, *2*, 19–21.

Wishnow, E. H., H. P. Gush, and L. Ozier (1996), Far-infrared spectrum of N_2 and N_2-noble gas mixtures near 80 K, *J. Chem. Phys.*, *104*, 3511–3516.

Wunch, D., G. C. Toon, J.-F. L. Blavier, R. A. Washenfelder, J. Notholt, B. J. Connor, D. W. T. Griffith, V. Sherlock, and P. O. Wennberg (2011), The total carbon column observing network, *Philos. Trans. Roy. Soc. A*, *369*, 2087–2112.